

Landslide susceptibility analysis using frequency ratio and weight of evidence approaches along the Lakhandehi Khola watershed in the Sarlahi District, southern Nepal

Anup Neupane, Kabi Raj Paudyal*, Krishna Chandra Devkota, Pratiksha Dhungana

Central Department of Geology, Tribhuvan University, Kathmandu, Nepal

*Corresponding email: paudyalkabi1976@gmail.com

Received: 30 October, 2022; Accepted: 05 November, 2022; Published :March,2023

Abstract

Landslide susceptibility maps are considered as one of the most important keys to limiting and dodging potential landslide consequences worldwide. In the present study, landslide susceptibility maps are prepared using bivariate models: frequency ratio and weight of evidence approaches. At first, randomly selected 80% of landslides i.e., one hundred eighty landslides are used as training data for the preparation of the model, and the rest 20% of landslides i.e., forty-five landslides for its validation. Similarly, thematic layers of nine causative factors of landslides such as slope, aspect, curvature, stream density, TWI (Topographic Wetness Index), land use, geology, distance from river and distance from the road have been analyzed for the modeling in ArcGIS. Finally, prepared landslide susceptibility maps are classified into five classes from Very Low to Very High from both methods. The area of Low, Moderate, High, and Very High susceptible classes is also nearly equal. The success rate curve of FR (Frequency Ratio), and WOE (Weight of the Evidence), show accuracy of 71.09%, and 75.62% respectively. Likewise, the prediction rate curve shows 72.87% and 76.66% accuracy on FR and WOE methods respectively. Since the susceptibility maps prepared through both approaches show an accuracy of >70%, the result is deliberated as fair. These maps are useful to all the stakeholders for land use planning and developing mitigation strategies against the consequences of increasing landslides in the Siwalik Hills of Nepal.

Keywords: Landslide susceptibility, frequency ratio, weight of evidence, lithology, Lakhandehi Khola

Introduction

In hilly landscapes like Nepal Himalayas, landslides are one of the most alarming natural hazards. Due to Nepal's unstable geological conditions, lateral variations in geomorphology, and climatic conditions (heavy rainfall) the risk of a landslide is higher (Upreti & Dhital 1996, Dhital 2000, Pathak 2016). It's common and often frequent in places like in the Siwalik Hills, where the lithology is fragile, and the topography is rugged with an active tectonic zone (Dahal *et al.* 2008, Neupane & Paudyal 2021). Several weaker geological conditions: for example, the harder sandstones inter-bedded with softer mudstone beds, the occurrence of differential weathering in sandstone and mudstone (Dahal *et al.* 2012, Bhandari & Dhakal 2018), loosely cemented conglomerate beds, and permeable Quaternary deposits on different slope angles (Bhandari & Dhakal 2018) are responsible for occurrences of landslides in the Siwalik region of Nepal.

It is well-accepted worldwide that landslide threat can be successfully alleviated with a precise understanding of the geology, and the anticipated frequency, character, pattern, and magnitude of slope failures in each location. Since the landslide susceptibility map portrays the likelihood of future landslides in the concerned area, it is one of the most important keys to minimize landslide consequences. This study aims to prepare a landslide susceptibility map using ArcGIS, following bivariate statistical models such as frequency ratio and weight of evidence methodology. This map exhibits the present landslide susceptibility zones and the probability of future occurrences of landslides which is useful to all the stakeholders for land use planning and developing mitigation strategies against the consequences of increasing landslides in the Siwalik Hills of Nepal Himalaya. The results of the susceptibility mapping can be used to plan and prioritize effective disaster risk reduction strategies (Paudyal *et al.* 2021).

Study area

Geographically, the study area is located between 27°3'0.79"N and 85°34'13.88"E to 27°11'10.58"N and 85°45'0.90"E co-ordinates. The study area is outlined from the parts of five toposheets of scale 1:25,000. They are Nepani (2785 16A), Khayarsal (2785 15B), Hariaun (2785 15C), Lalbandi (2785 15D), and Pantale (2785 15A). The rugged topography of the LakhandehiKhola watershed area differs from steep slopes (>45°) to gentle slopes (<7°) in the Siwalik area. The lowest elevation of the study area is 181 m at the Betali Khola in the western most part of the study area, whereas the highest elevation is 706 m at Baunechuri in the southern part of the study area. The climate of the Lakhandehi Khola watershed belongs to the monsoon subtropical zone and can be divided into two separate seasons as the dry seasons (October to May) and the wet seasons (June to August). The yearly average temperature is 25°C, with the coldest month being 8.90°C and the hottest month being 30.8°C. January is the coldest month,

and May and June are the hottest months. The monsoon season occurs in the study area from June to September. A study of rainfall and temperature data from 1988 to 2017 revealed that the study area's mean monthly rainfall decreased by 2.57 mm per year and the summer temperature increased by 0.024°C per year (Bhandari *et al.* 2021). The location map of the present study area is shown in Figure 1.

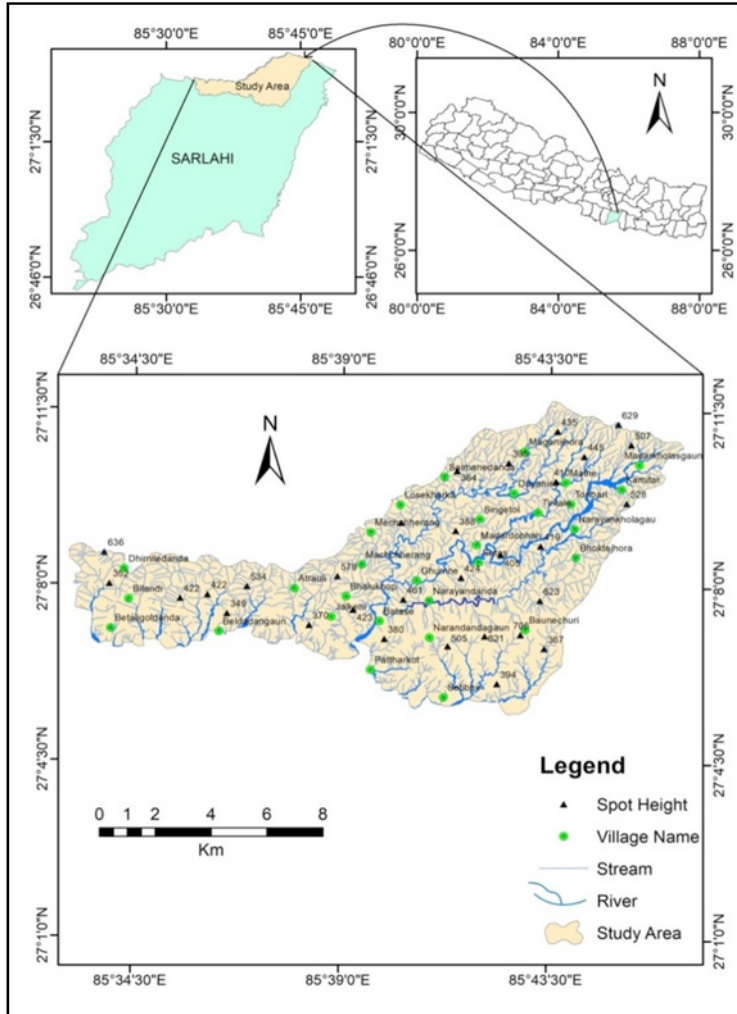


Figure 1: Location map of the study area.

Geological setting

Geologically, the study area is situated in the Siwalik zone of Nepal Himalaya, stretching immediately north from the Main Frontal Thrust (MFT) at Pattharkot Village.

The Siwalik in Nepal is characterized by the presence of sedimentary rocks such as shale, mudstone, sandstone, and conglomerate in various proportions (Dhital 2015, Sah 1999, Thakur 2001, Upreti 2001). Considering the lithological contrast, color, and thickness, the rock units in the study area are classified into four parts (Figure 2): the Lower Siwalik, the lower Middle Siwalik (MS1), the upper Middle Siwalik (MS2), and the Upper Siwalik (Neupane & Paudyal 2021). In this region, medium-to thick-bedded, variegated mudstone and sandstone belong to the Lower Siwalik, thick-bedded, fine-to coarse-grained salt-and-pepper types of sandstone belongs to the Middle Siwalik and pebble-cobble conglomerate belongs to the Upper Siwalik. The beds are gently to steeply dipping towards NE and NW.

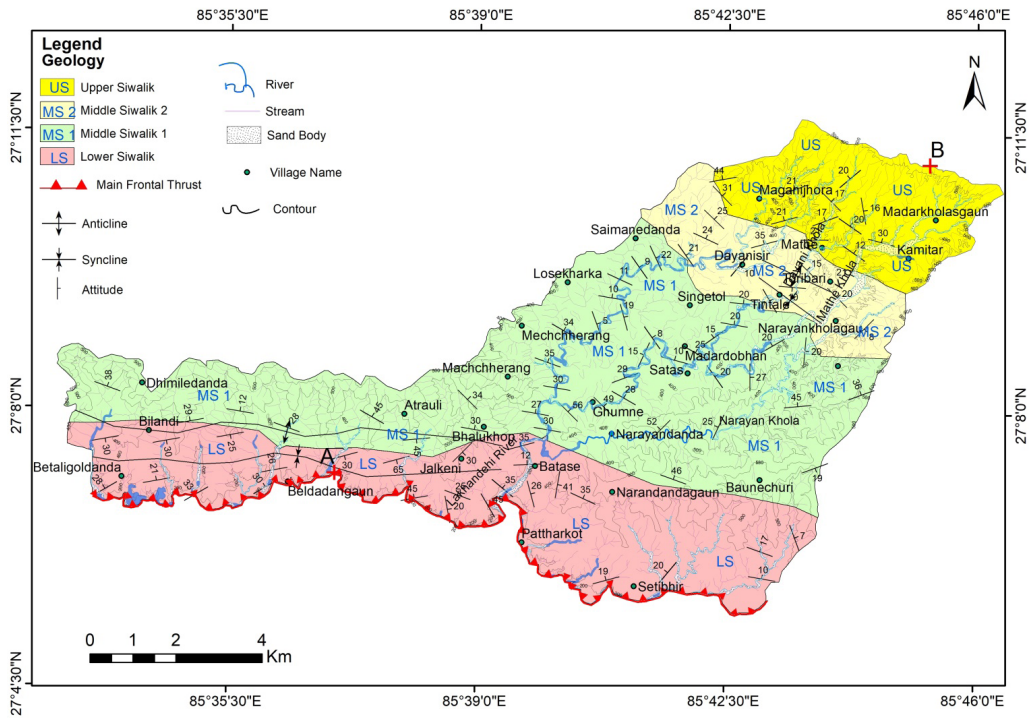


Figure 2: Geological map of the study area.

Landslide inventory map

The main purpose of the landslide inventory is to acquire an overview of the area impacted by landslides, mass movements, and large to small-scale erosion. The crucial information on the existing scenario of landslides, such as their distribution, patterns, frequency, cause of landslides, etc. could also easily be accessed through such maps (K.C. et al 2018). Landslide signals such as morphological deformities, bending of trees, and bare terrain were also thoroughly explored. During this inventory, landslides

were easily identified by their ongoing processes with fresh scarps, rock cliffs, barren vertical multi-storied beds, and landslide materials. Moreover, scarps and evidence observed on the computer tool Google earth pro-2017 over the last 25 years were also considered active landslides. In this study, polygons were made in every landslide from the computer tool Google EarthPro 2017 and verified in the field (Figure 3).

All together 225 landslides were identified in approximately 109.6 km² of the study area. The inventory was limited to the foot trails, along river sections and residential areas. Landslides that are in inaccessible regions were identified from the computer tool “Google earth pro-2017”. All these landslides were converted into the raster format with a pixel size of 12.5×12.5 m. The area of the landslides ranges from 113.176 m² to 923561.983 m². Out of the 109.6 km² of the area of the Siwalik section of the Lakhandehi Khola watershed, landslides accounted for 0.780 square meters, making landslides’ density 71%. This indicates the severe impact of landslides in the study area. For the assessment of landslide susceptibility, randomly selected 80% landslides i.e., one hundred eighty landslides were used as training data for the preparation of the model, and the rest 20% landslides i.e., forty-five landslide data were taken for its validation or to determine its success rate.

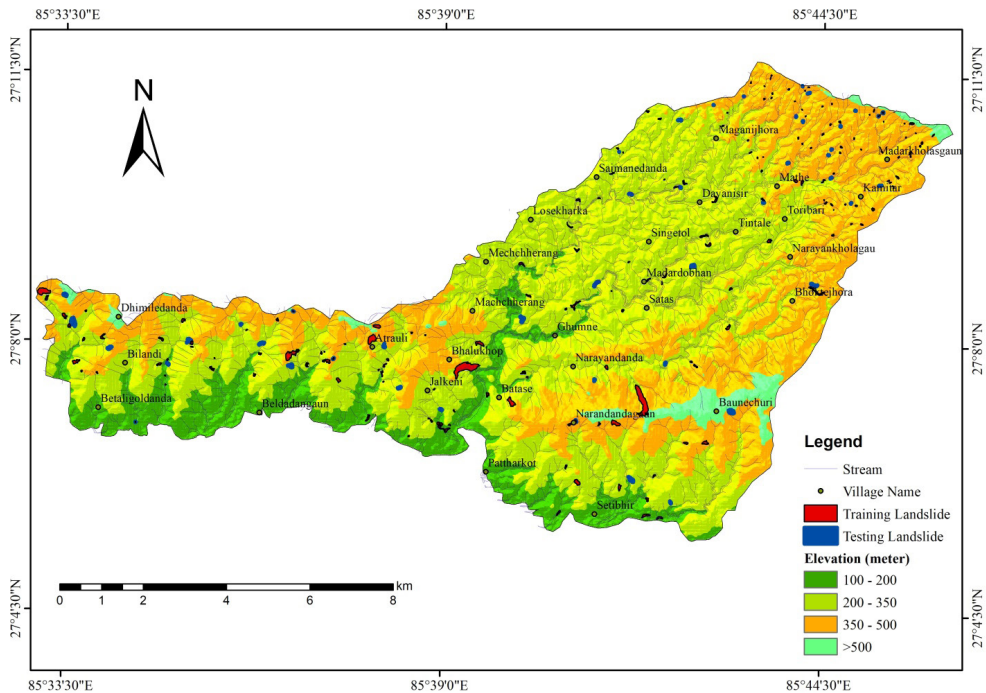


Figure 3: Landslide inventory map of the study area

Landslides conditioning factors

For landslide susceptibility assessment, 4 major causative factors enhancing landslides were identified in the field. They were geological, anthropogenic, hydrological, and geomorphological. Geological factors include lithological control over landslides. Anthropogenic activities are ongoing human activities such as the construction of roads, land use, etc. A hydrological factor comprises the topographical wetness index, distance from the river, and drainage density. Finally, geomorphologic factors include slope, curvature, and aspect. Thus, altogether nine thematic GIS layers were cast off for the modeling. All data was resampled to roughly 12.5×12.5 m resolution and projected onto the "UTM 45" (Universal Transverse Mercator) datum/coordinate system.

Slope

The slope of any area symbolizes the angle of the steepness of the landscape and is considered one of the major important factors for landslide manifestation. Slope failure due to the slope is caused mainly due to interchange in shear stress with gradient under the influence of gravity. Moreover, permeability, cohesion, and other material property also alter with slope gradient. Sliding action or mass wasting is more prominent on steep slopes than on gentle ones. The research area's slope map is derived from the DEM map with a resolution of 12.5×12.5 m using the "Raster Surface". The slope angle obtained in the study area ranged from 0° to 70.8108°. This value is classified into six different categories as: 0-5°, 5-10°, 10-15°, 15-25°, and >25°(Figure 4).

Aspect

Aspect, in general, refers to the position of the topography in a certain direction. The aspect of certain landscapes also plays an important role in landslide occurrences as it governs the amount of the soil moisture content in an area being influenced by processes such as evapotranspiration, rainfall, sunlight, wind impacts, and so on. The amount of sunshine that reaches the area, as well as seepage and groundwater conditions, is all influenced by the slope's aspect (Hamza & Raghuvanshi 2017). These processes also severely impacted weathering and vegetation root development in plants. However, many scientists argue the role of the slope aspect as a major factor that determines the occurrences of landslides. In this study, the "Raster Surface" in the GIS was used to create an Aspect map from the DEM map of 12.5×12.5 resolutions. The slope aspect of the study area ranges from a categorical value of -1 to 359.524. This value represents the angle in degrees demonstrating the direction of the slope which is further divided into nine different classes as: Flat, north-east, east, south-east, south, south-west, west, north-west, and north (Figure 5).

Curvature

In landslide and geomorphology, curvature refers to the curve features of the landscapes. Mostly, the curvature can be classified into three classes: concave, planer, and convex.

Curvature impact the occurrence of landslides as the distribution of the surface and subsurface water on the slope is reliant on its shape. In this study, the "Raster Surface" in the GIS was used to create a curvature map from the DEM map of 12.5×12.5 resolutions. The planform curvature values in the study area range from -9.62207 to 8.074. This categorical value is further divided into three different classes: Concave, Flat, and Convex (Figure 6). The concave curvature feature class represents all the positive values, the concave features class represents all the negative values and flat features represent zero values or it is indicating planer surfaces.

Stream density

Drainage Density is calculated by dividing the total length of all streams and rivers in a drainage basin by the drainage basin's entire area. The study terrain's topography is complex, since it is heavily dissected by multiple streams and tributaries, and it features stiff and overhanging slopes in certain places. For the landslide susceptibility assessment stream density in the present study area is obtained from the line density of the spatial analyst tool based on stream order. The numeric field denoting population values (the number of times the line representing the overall order of stream should be counted) for each polyline is the basis of obtaining stream density. The stream density value obtained from the ratio of the sum of all lengths of streams to the total area of the Siwalik section of the Lakhandehi Khola watershed is 5.15056 km/km². This categorical variable value indicates high Stream density. The stream density value in the study area ranges from 0 to 31.3308. This value is further classified into three categories as (0-7), (7-13), and (>13) indicating Low, Medium, and High-density classes respectively (Figure 7).

Topographic wetness index (TWI)

The wetness index, developed by the United States Geological Survey also provides an indicator of groundwater potential. It is currently being used in landslide susceptibility assessments as the key causal component. The regional distribution and spatial proportions of the area of relative wetness and area of relative dryness are provided by the wetness index. Generally, TWI is expressed as:

$$TWI = \ln (\alpha / \tan \beta),$$

where, α is the cumulative upslope area draining through a point (per unit contour length), $\tan \beta$ is the slope angle at the point.

The relative value of TWI varies from 1.66155 to 20.5955 in the study area. These values are classified further into five different classes: (1-4), (4-6), (6-8), (8-12.5), and (>12.5) (Figure 8).

Land use or land cover

Land use or land cover configuration is also one of the major influencing factors in enhancing landslides. In the study area, four types of Land use or Land cover patterns were seen. They are forests, settlements/cultivations, rivers, and sand bodies (Figure 9). There is a high risk of landslides in the loose and bare soil of settlements/cultivation areas. Rivers also enhance landslides by toe-cutting of slopes. Similarly, plant roots may cause fissures in the underlying substrate, increasing the likelihood of a landslide. The Land use map in this study was prepared by digitizing the topographical maps and was verified using the Google earth pro-2017 tool to minimize errors by depicting the present scenario in the study area.

Geology

Because different geological units have different susceptibilities to active geomorphological processes, geology plays a significant role in landslide susceptibility and hazard research (Pardhan *et al.* 2002, Timalina & Paudyal 2021). The risk of landslides is more in active and fragile terrain such as Siwalik Hills (Dahal *et al.* 2012, Pokhrel 2013, TU-CDES 2016, Dahal & Paudyal 2022). Lithology has a strong influence on the kind, size, and distribution of landslides in the Siwalik range (Neupane & Paudyal 2021). Initially, a geological map was prepared over the topographical map in the field which was later digitized in the ArcGIS tool using polygon features for different Formations, and finally, it was converted to a raster of pixel 12.5*12.5 m for landslide susceptibility assessment. The geology of the present study area is divided into four geological units as the Lower Siwalik, lower Middle Siwalik (MS1), upper Middle Siwalik (MS2), and the Upper Siwalik from older to the younger unit, respectively (Figure 2).

Distance from road

Road distance is also one of the important causative factors considered in the occurrences of landslides. The field study revealed that haphazard road excavation without the consideration of geological and geotechnical features has caused shallow landslides (Budha *et al.* 2016, Shahi *et al.* 2022). The haphazard and unmanaged constructions of the roads built on the slopes cause the loss of support and bring changes in topography causing loss of support which ultimately leads to the increase of strain behind the slope and the development of cracks. Moreover, water infiltration in poorly managed drainage in any road section causes aid to slope failure. Distance from the road in this study was prepared using the Euclidian distance tool of the newly digitized polyline layer of roads from the topographical map and Google earth Pro 2017. In the study area, poor alignment profile, absence of proper drainage management, use of wrong construction material, lack of drainage management, and total absence of maintenance and reconditioning

procedures of roads were observed along the newly constructed roads causing landslides. This is most serious on the newly constructed roads from Patharkot to Narayandanda and many other sections. The categorical value of the distance from the road is obtained from 0 to 1755.39 in the study area. This value is buffered at various intervals such as 0-100, 100-250, 250-500, 500-1000, and >1000 meters (Figure 11).

Distance from river

Rivers are responsible for generating landslides in terrain with soft lithology like Siwalik, eroding the toe, and adding water to the nearby slope. Thus, river buffers were used in this study. It was prepared from a newly digitized polyline layer of rivers from the topographical map using the Euclidian distance tool. In the study area, the distance from the river categorical value was obtained from 0 to 2048.55. This categorical value was further divided into five different classes 0-150, 150-250, 250-350, 350-500, and >500 meters (Figure 12).

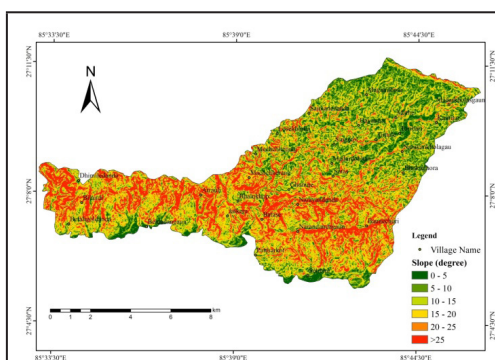


Figure 4: Slope map of the study area

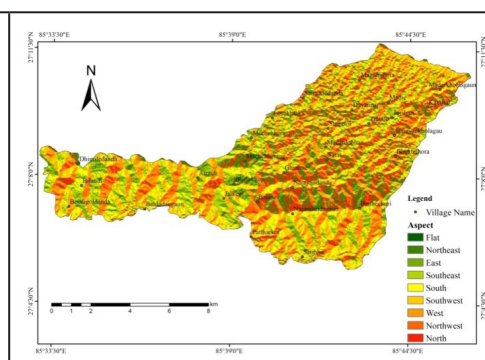


Figure 5: Aspect map of the study area

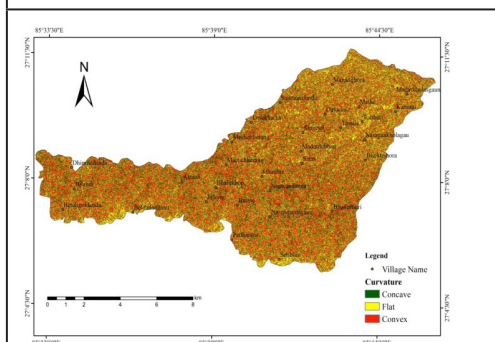


Figure 6: Curvature map of the study area

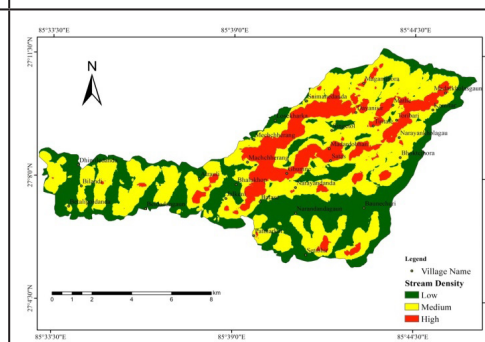


Figure 7: Stream Density map of the study area

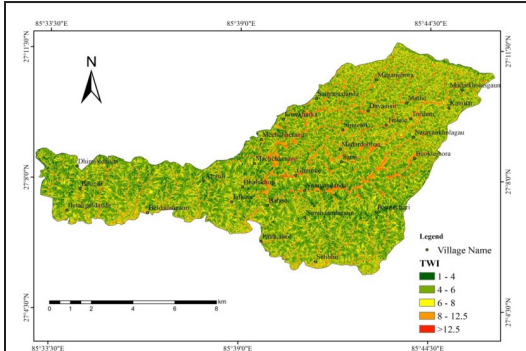


Figure 8: TWI map of the study area

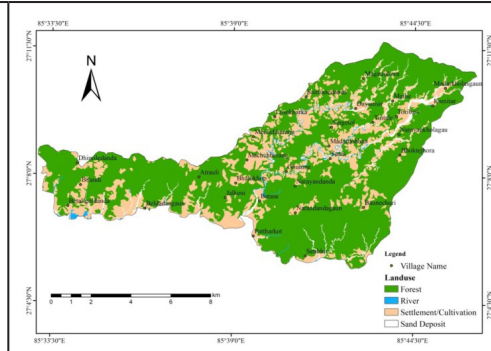


Figure 9: Land-use map of the study area

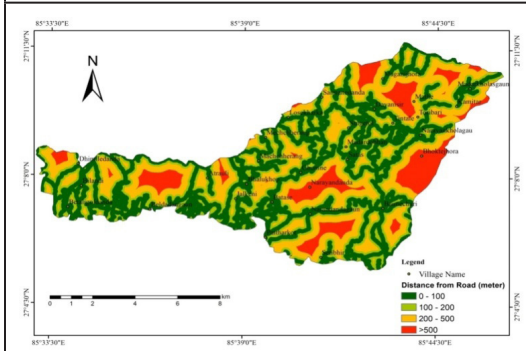


Figure 10: Distance from road map of the study area

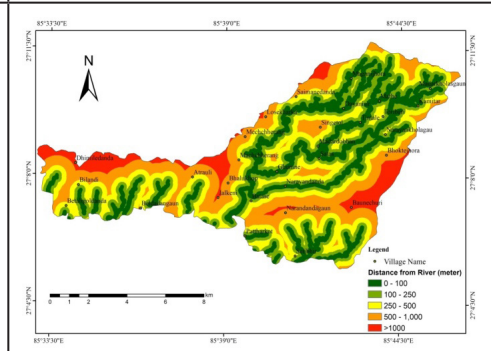


Figure 11: Distance from river map of the study area

Modeling approach

In the modern era, numerous techniques have been developed worldwide for the assessment of landslide susceptibility. Devkota *et al.* (2012), mentioned that the efficiency of landslide susceptibility assessment using GIS and statistics is dependent on the proper selection of the parameters that influence slope stability. They generated the landslide susceptibility map of the Mugling–Narayanghat road section using certainty factor, index of entropy, and logistic regression by evaluating causative factors such as slope gradient; slope aspect; altitude; plan curvature; lithology; land use; distance from faults, rivers, and roads; topographic wetness index; stream power index; and sediment transport index with their developed model to be greater than 80% accurate. Regmi *et al.* (2014), applied frequency ratio, statistical index, and weights-of-evidence models to study landslide susceptibility through comparison in Central Nepal. They concluded with the findings that the FR model, with a success rate of 76.8% and predictive accuracy

of 75.4% outperforms the WoE (success rate, 75.6%; predictive accuracy, 74.9%) in their study area.

Amongst all the techniques, statistical analysis methods are applied for the landslide susceptibility assessment in the present study. Statistical methodologies can be reliably divided into bivariate statistics and multivariate statistics amongst which the bivariate statistics approach is applied in this study. The inductive logic that underpins the bivariate statistical approach is that if a scenario is true for all the observed examples, it is likewise true for all other circumstances (Shano *et al.* 2020). Therefore, these methods are predicated on the axiom that "past and present is the key to the future" (Dai & Lee 2001). Out of numerous bivariate statistical approaches, Frequency Ratio and Weight of Evidence methodologies are applied for landslide susceptibility assessment in the present study.

Methodology applied using frequency ratio approach

It is one of the crucial probability methods in landslide susceptibility assessment as it correlates the landslides between the distribution of landslides and each conditioning factor associated with landslides. It is the ratio between the probability of a landslide occurring and not occurring in each certain area (Lee & Talib 2005).

The frequency ratio (FR) can be expressed as:

$$FR = (\% X / \% Y)$$

Where "X" is the percentage of landslides in a causative factor class and "Y" is the area of the causative factor class as a percentage of the entire map".

The landslide susceptibility index can be generated by the summation of each factor's FR value as:

$$LSI = \sum FR$$

"If the ratio is greater than 1, the relationship between a landslide occurrence and the specific factors attributes; and if it is less than 1, the opposite is true (Regmi *et al.* 2014)".

The relative frequency is calculated as:

$$RF = FR_i / \sum_{n=1}^i FR$$

Where, FR_i = Frequency Ratio of each class of a factor and $\sum_{n=1}^i FR$ is the summation of the Frequency Ratio of each class.

Similarly, the prediction rate is computed as:

$$PR = (\text{Max}_{RF} - \text{Min}_{RF}) / (\text{Max} - \text{Min})_{\text{MinRF}}$$

Where, Max_{RF} and Min_{RF} are the maximum and minimum relative frequencies respectively, and $(\text{Max} - \text{Min})_{\text{MinRF}}$ is the minimum relative frequency of subtraction of Min_{RF} from Max_{RF} . For the landslide susceptibility assessment using the Frequency ratio technique, the following equation was derived to prepare a landslide susceptibility index map which was applied using the raster calculator tool in ArcGIS.

$$LSI = 9.57 \times F_{\text{slope}} + 3.76 \times F_{\text{Aspect}} + 5.59 \times F_{\text{Curvature}} + 1.00 \times F_{\text{Distance from Road}} + 1.01 \times F_{\text{Distance from River}} + 3.01 \times F_{\text{Geology}} + 4.70 \times F_{\text{Landuse}} + 2.23 \times F_{\text{Stream Density}} + 3.81 \times F_{\text{TWI}}$$

A brief explanation of the causative factor their calculated FR value and prediction ratio is represented in Table 1. The landslide susceptibility index map that shows stretched categorical values ranging from Low: 424.616 to High 1272.59 is presented in Figure 13. This value was further classified into five classes: Very Low, Low, Moderate, High, and Very High using the natural break method and is shown in Figure 15.

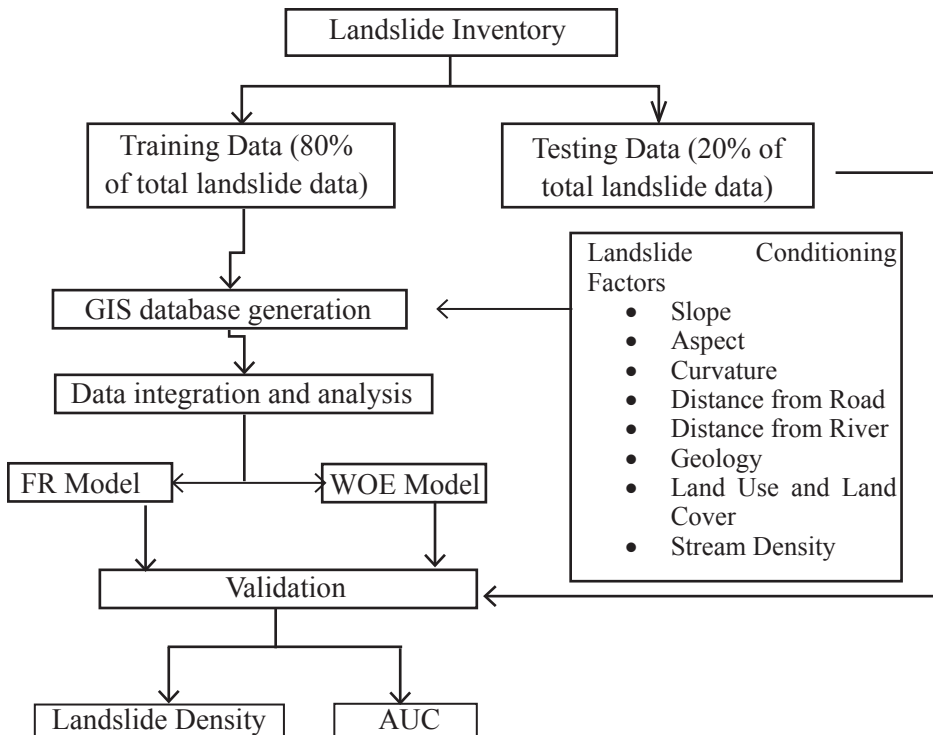


Figure 12: Flowchart showing the methodology adopted in this study.

Table 1: FR and PR weightage for landslide susceptibility of different parameters for frequency ratio approach

Factor	Class	Total pixel in class	Pixels of landslides in that class	Frequency ratio (FR)	relative frequency (RF)	PR
Slope	0-5	66354	127	0.31	0.05	9.57
	5-10	137057	299	0.36	0.06	
	10-15	146178	397	0.44	0.08	
	15-20	137665	563	0.67	0.11	
	20-25	93950	777	1.35	0.23	
	>25	119814	2124	2.90	0.49	
Aspect	Flat (-1)	1911	1	0.09	0.01	3.76
	North (0-45)	68644	173	0.41	0.05	
	Northeast (45-90))	62775	310	0.81	0.10	
	East (90-135)	94978	764	1.32	0.17	
	Southeast (135-180)	110719	968	1.43	0.18	
	South (180-225)	104678	627	0.98	0.13	
	Southwest (225-270)	103323	515	0.82	0.10	
	West (270-315)	84951	519	1.00	0.13	
Northwest (315-360)	69039	410	0.97	0.12		
Curvature	Concave	176529	1384	1.28	0.42	5.59
	Planer	218666	668	0.50	0.16	
	Convex	305823	2235	1.20	0.39	
Distance from road (meter)	0 - 100	262317	1684	1.05	0.27	1.01
	100 - 250	152530	948	1.02	0.26	
	250 - 500	202850	1209	0.98	0.25	
	>500	83734	446	0.87	0.22	
Distance from the river (meter)	0-100	152073	1044	1.12	0.23	1
	100-200	155093	879	0.93	0.19	
	200-350	174041	952	0.90	0.18	
	350-500	163203	1088	1.09	0.22	
	>500	57044	324	0.93	0.19	
Lithology	Lower Siwalik	204298	1160	0.93	0.29	3.01
	Lower Middle Siwalik	334639	2293	1.12	0.34	
	Upper Middle Siwalik	72004	297	0.67	0.21	
	Upper Siwalik	90077	537	0.97	0.30	
Landuse and land cover	Forest	507637	3492	1.13	0.33	4.70
	Settlement	165533	692	0.68	0.20	
	Sand Deposit	21938	58	0.43	0.13	
	River	6323	45	1.16	0.34	
Stream density	Low	261984	1887	1.18	0.39	2.23
	Medium	335607	1787	0.87	0.29	
	High	103863	613	0.97	0.32	
TWI	<4	232157	1868	1.32	0.31	3.81
	4 - 6	292222	1629	0.91	0.21	
	6 - 8	114141	565	0.81	0.19	
	8 - 12.5	50758	178	0.57	0.13	
	>12.5	11740	47	0.65	0.15	

Methodology applied using weight of evidence approach

The weight of the Evidence approach is based on the notion that landslide causative variables may be quantified by determining each class's landslide densities. The landslide densities within each parameter map or causative variables and their classes are used to calculate weight values for those classes in this approach. The landslide susceptibility map is created by combining these weighted parameter maps. The outcome of bivariate analysis methods is determined by the parameters or causative factors for slope instability that are chosen. At first, positive and negative weight values of each factor were calculated using the mathematical formulation of weight based on (Dahal *et al.* 2008, Regmi *et al.* 2014):

$$W^+ = \ln(\text{area in class} / N_{\text{pix total landslide area}}) / \ln(N_{\text{pix stable area in class}} / N_{\text{pix total}})$$

$$W^- = \ln(\text{area outside class} / N_{\text{pix total landslide area}}) / \ln(N_{\text{pix stable area outside class}} / N_{\text{pix total}})$$

Here, W^+ signifies the event occurrences, and W^- signifies the event non-occurrences. Moreover, it must be noted that pixel numbers should be input values. Now, a particular class weight value was calculated using the equation

$$W_j = \sum_{i=1}^n W_i$$

Where W_j is a class parameter and W_i describes positive and negative values of the weight. In this method factors controlling landslides can be mapped:

Finally, weightage can be used to contrast value (C) is defined by the equation:

$$C = W^+ - W^-$$

Where $C = 0$ represents the affecting factor that is not significant for the analysis.

For predicting the total landslide susceptibility index for the single pixel all the predictive values are combined numerically as follows.

$$W_{ij} = W_{\text{slope}} + W_{\text{aspect}} + W_{\text{curvature}} + W_{\text{geology}} + W_{\text{landuse}} + W_{\text{twi}} + W_{\text{streamdensity}} + W_{\text{distance from river}} + W_{\text{distance from road}}$$

Where W_{ij} is the Landslide susceptibility index. This was calculated in ArcGIS using the raster calculator tool. The landslide susceptibility index map that shows stretched categorical values ranging from Low: -6.40456 to High 4.86316 in the study area is presented in Figure 14. This value was further classified into five classes Very Low, Low, Moderate, High, and Very High using the natural break method and is shown in Figure 16.

Table 2: Landslide Susceptibility weightage of different parameters for the WOE approach

Factor	Class	Total pixel	Pixel of landslide in class	W+	W-	Total
Slope	0-5	66354	127	-1.17	0.07	-1.24
	10-15	146178	397	-1.03	0.15	-1.18
	15-20	137665	563	-0.82	0.14	-0.95
	20-25	93950	777	-0.40	0.08	-0.48
	>25	119814	2124	0.30	-0.06	0.36
	10-15	146178	397	1.08	-0.50	1.58
Aspect	Flat (-1)	1911	1	-2.46	0.00	-2.47
	North (0-45)	68644	173	-0.89	0.06	-0.95
	Northeast (45-90))	62775	310	-0.21	0.02	-0.23
	East (90-135)	94978	764	0.28	-0.05	0.33
	Southeast (135-180)	110719	968	0.36	-0.08	0.44
	South (180-225)	104678	627	-0.02	0.00	-0.02
	Southwest (225-270)	103323	515	-0.21	0.03	-0.24
	West (270-315)	84951	519	0.00	0.00	0.00
Northwest (315-360)	69039	410	-0.03	0.00	-0.03	
Curvature	Concave	176529	1384	0.25	-0.10	0.35
	Planer	218666	668	-0.70	0.21	-0.90
	Convex	305823	2235	0.18	-0.16	0.34
Distance from road (meter)	0 - 100	262317	1684	0.05	-0.03	0.08
	100 - 250	152530	948	0.02	0.00	0.02
	251 - 500	202850	1209	-0.03	0.01	-0.04
	>500	83734	446	-0.14	0.02	-0.16
Distance fromriver (meter)	0-100	152073	1044	0.12	-0.03	0.15
	100-200	155093	879	-0.08	0.02	-0.10
	200-350	174041	952	-0.11	0.03	-0.15
	350-500	163203	1088	0.09	-0.03	0.12
	>500	57044	324	-0.07	0.01	-0.08
Lithology	Lower Siwalik	204298	1160	-0.07	0.03	-0.10
	Lower Middle Siwalik	334639	2293	0.11	-0.12	0.23
	Upper Middle Siwalik	72004	297	-0.40	0.04	-0.43
	Upper Siwalik	90077	537	-0.03	0.00	-0.03
Land Use and Land Cover	Forest	507637	3492	0.12	-1.22	1.34
	Settlement	165533	692	-0.38	-0.04	-0.34
	Sand Deposit	21938	58	-0.84	-0.09	-0.75
	River	6323	45	0.15	-0.11	0.27
Stream Density	Low	261984	1887	0.17	-0.11	0.28
	Medium	335607	1787	-0.14	0.11	-0.25
	High	103863	613	-0.04	0.01	-0.04
TWI	<4	232157	1868	0.28	-0.17	0.45
	4 - 6	292222	1629	-0.09	0.06	-0.15
	6 - 8	114141	565	-0.21	0.04	-0.25
	8 - 12.5	50758	178	-0.56	0.03	-0.59
	>12.5	11740	47	-0.43	0.01	-0.43

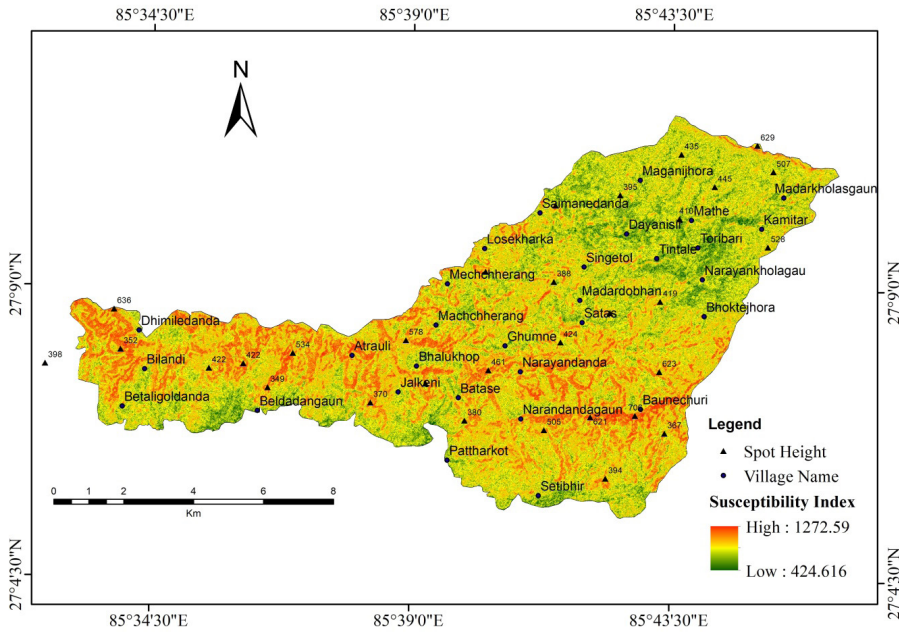


Figure 13: Landslide susceptibility map prepared using FR approach of the study area.

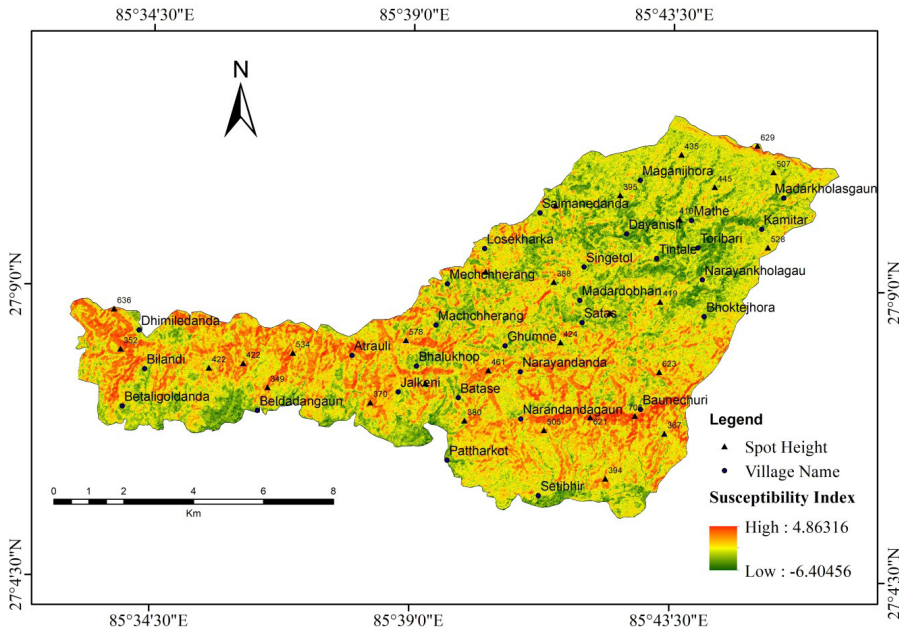


Figure 14: Landslide susceptibility map prepared using the WOE approach of the study area.

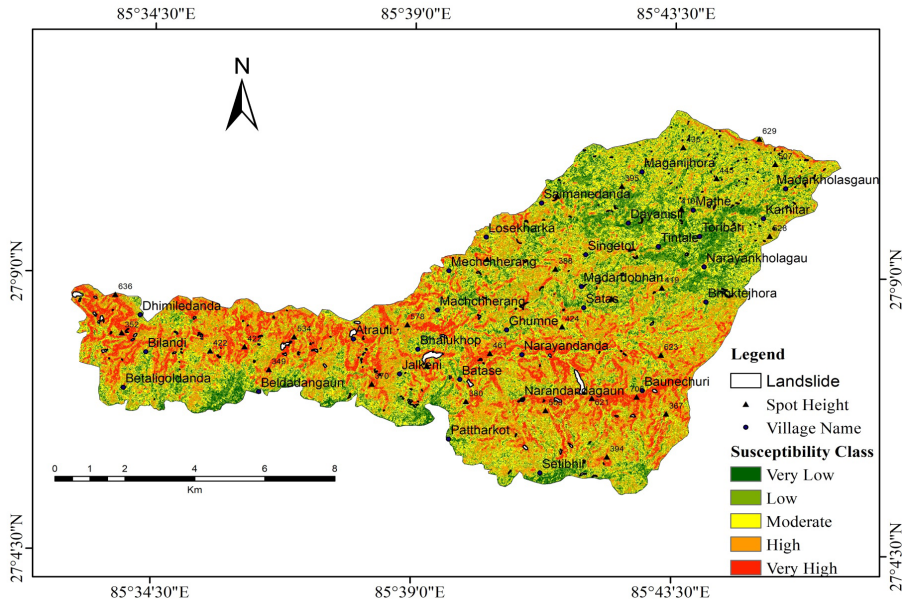


Figure 15: Classified landslide susceptibility map prepared using FR approach of the study area.

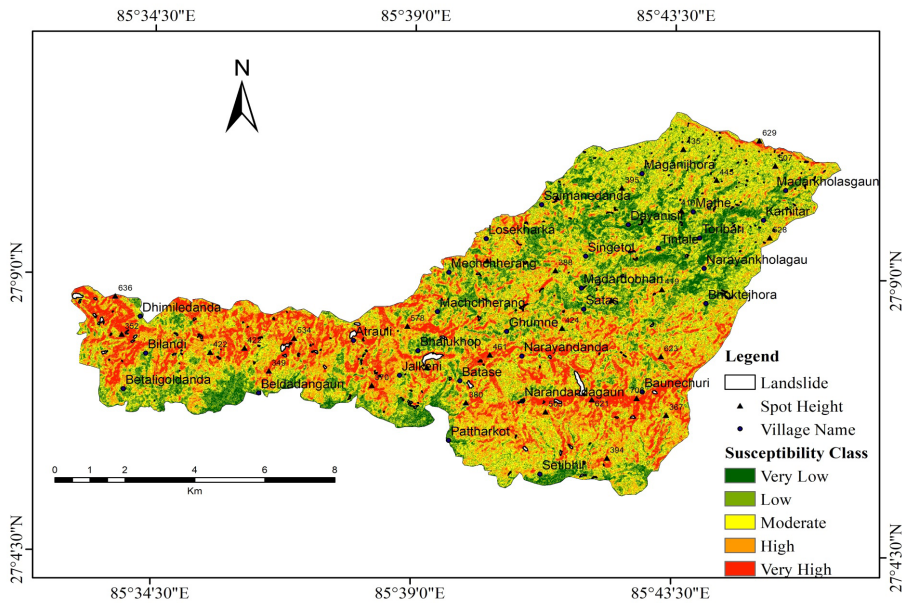


Figure 16: Classified landslide susceptibility map prepared using the WOE approach of the study area

Discussions

Discussion on landslide susceptibility maps

Landslide susceptibility maps were prepared in this study using two of the bivariate methodologies, i.e., using Frequency Ratio and Weight of Evidence methodologies. These maps were classified into five classes as: Very Low, Low, Moderate, High, and Very High using the natural break methods. It was observed that the Middle Siwalik section of the study area shows high and very high susceptibility zone and in other geological units, susceptibility classes are nearly equally distributed. Villages such as Losekharka, Bhalukhop, Narayandanda, Atrauli, and Baunichuri. are high to very highly susceptible to landslides, and villages such as Narayankholagaun, Kamitar, Tintale, and Patharkot are least susceptible to landslides.

Comparison based on landslides density and landslide area

Landslide density is generally calculated by calculating the ratio of the area of a certain susceptible class to the area of landslides in a certain class. It was observed that the different susceptible zones classified in both methods are almost equal in area. Thus, in terms of the landslide area, both methods showed excellent results which amplified the reliability and validation of both models in terms of landslide susceptibility zonation. The observed landslide densities within the area of this study are represented in Table 3. It was also observed that in both methods' landslide densities are progressively increasing from Very Low to Very High susceptible class (Figure 17 and Figure 18) which also validates the susceptibility class zonation of this study.

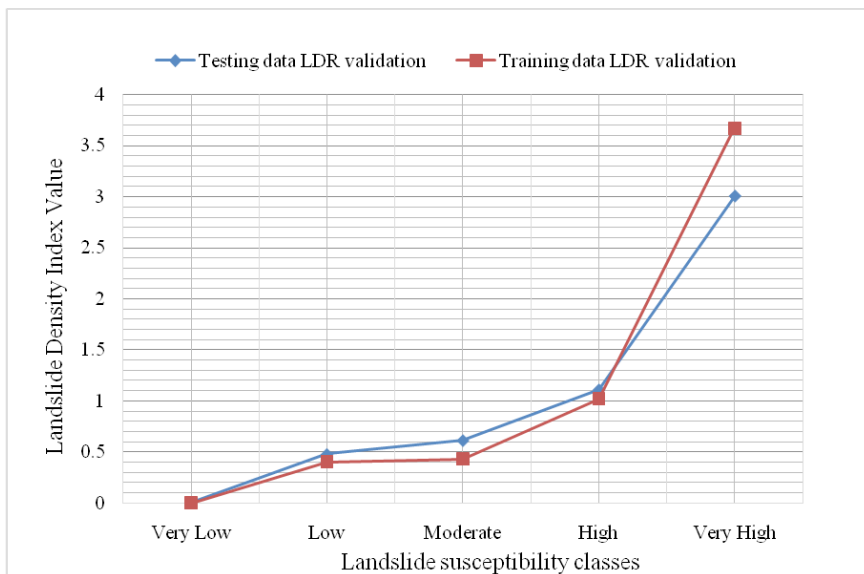


Figure 17: LDR validation from Frequency Ratio method of the study area.

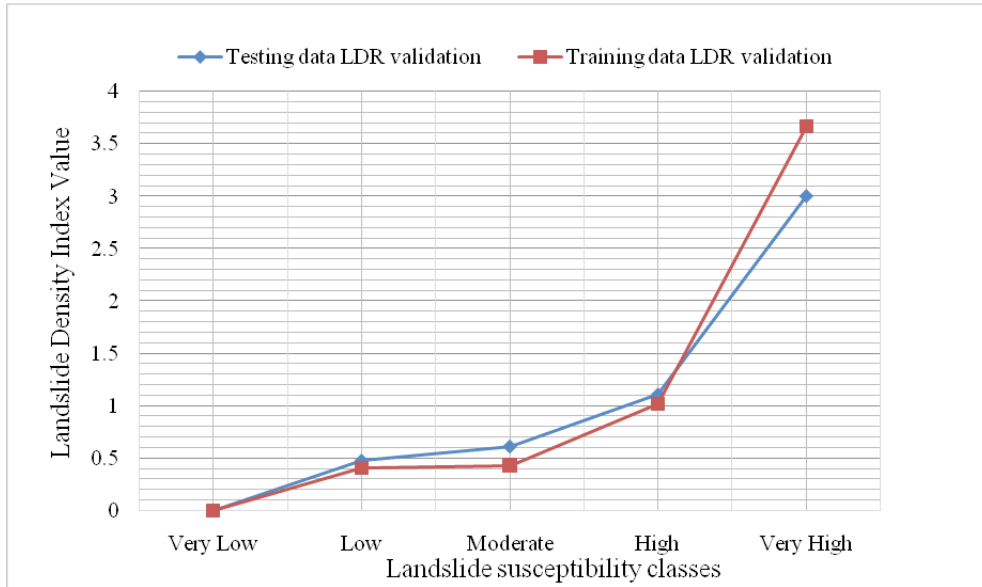


Figure 18: LDR validation from the WOE method of the study area.

Table 3: Comparison based on landslide density

Susceptibility zones	Weight of evidence (WOE)			Frequency ratio		
	Area (%)	Landslide (%)	Landslide density (%)	Area (%)	Landslide (%)	Landslide density (%)
Very Low	9.294	2.760	0.297	18.777	7.879	0.419
Low	23.311	10.822	0.464	23.732	11.648	0.490
Moderate	29.179	17.472	0.598	31.654	20.878	0.659
High	24.610	27.065	1.099	10.821	13.442	1.242
Very High	13.604	41.878	3.078	15.013	46.150	3.074

Comparison based on success rate curve

Another method of validating landslide susceptibility maps is evaluating the percentage of a landslide occurring in a certain susceptible zone i.e., through the preparation of the success rate. This technique is because high susceptibility zone must consist of more percentage of landslides as compared to other zones (Sarkar 2008). Thus, this is a qualitative technique to validate landslide susceptibility maps. The curve is obtained by plotting the cumulative percentage of observed landslide occurrences ordered from high to low in the x-axis and the Cumulative aerial percentage in decreased LSI value in Y axis. The curve prepared using training data (80% data) is considered as a success rate

curve and the curve prepared using testing data is considered a prediction rate curve. The success rate curve of FR and WOE shows an accuracy of 71.09% and 75.62%, respectively. Similarly, the prediction rate curve shows an accuracy of 72.87% and 76.66%, for FR and WOE methods, respectively (Figure 19). As the success rate and prediction rate of the landslide susceptibility zone using both techniques are above 70% which is satisfactory. Hence the maps produced in this study are fairly accurate. As the accuracy of WOE methods is higher, this method is reliable for further hazard zonation and risk assessment.

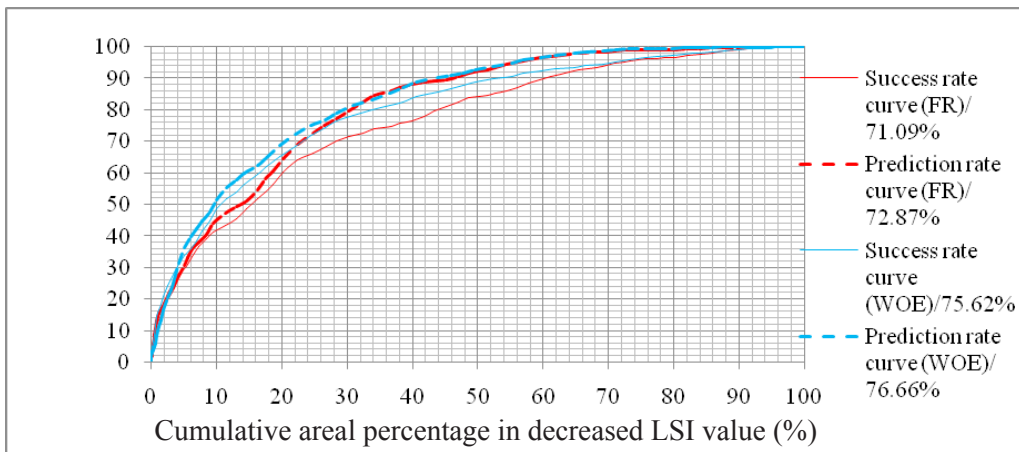


Figure 19: Success rate curve of LSZ maps of FR and WOE methods.

Conclusions

In this study, landslide susceptibility maps are prepared using bivariate models using frequency ratio and weight of evidence approaches. At first, randomly selected 80% of landslides i.e., one hundred eighty landslides have been used as training data for the preparation of the model, and the rest 20% of landslides i.e., forty-five landslides for its validation. Similarly, thematic layers of nine causative factors of landslides such as slope, aspect, curvature, stream density, TWI, land use, geology, distance from the river, and distance from the road were cast off for the modelling in ArcGIS. Finally, prepared landslide susceptibility maps are classified into five classes from very Low to Very High using the natural break method. In both methods, landslide densities are progressively increasing from Very Low to Very High susceptible class. The area of Low, Moderate, High, and Very High susceptible classes is also nearly equal. The success rate curve of FR and WOE shows an accuracy of 71.09% and 75.62%, respectively. Similarly, the prediction rate curve shows 72.87% and 76.66% accuracy for FR and WOE methods, respectively. Since the susceptibility maps prepared through

both approaches show an accuracy of >70%, the result is deliberated as fair. These maps are useful to all the stakeholders for land use planning and developing mitigation strategies against the consequences of increasing landslides in the Siwalik Hills of Nepal Himalaya. This research also endorses that even using currently accessible local data, a practical valid susceptibility map for landslide occurrence can be created.

Recommendations

This study is carried out in an approximately 110 km² area which is a regional scale. Although the results obtained in this study are valid, it is highly recommended to carry out further detailed studies on a small local scale using techniques such as deterministic and probabilistic approaches. Similarly, for a more effective result, consideration of other parameters which has a direct influence on landslides such as groundwater modeling, geological morpho-structural settings, soil depth, rainstorm, prolonged rainfall, seismic activity, etc. is highly recommended. The high to very high susceptible zone should be studied in detail and prevent the possible landslides consequences. In the future, landslides may occur in the low landslide susceptibility zones. Therefore, the landslide susceptibility map should be modified including the landslide data from the multiple events.

References

- Bhandari, R., Neupane, N. & Adhikari, D. P. (2021). Climatic change and its impact on tomato (*Lycopersicum esculentum* L.) production in plain area of Nepal. *J. Environmental Challenges* **4**. <https://doi.org/10.1016/j.envc.2021.100129>.
- Bhandari, B. P. & Dhakal, S. (2018). Lithological control on Landslide in the Babai Khola Watershed, Siwalik Zone of Nepal. *American Journal of Earth Sciences* **5**(3): 54-64.
- Budha, P. B., Paudyal, K. R & Ghimire, M. (2016). Landslide susceptibility mapping in eastern hills of Rara Lake, western Nepal. *Journal of Nepal Geological Society* **50**(1): 125–131. <https://doi.org/10.3126/jngs.v50i1.22872>
- Dahal, A. & Paudyal, K. R. (2022). Mapping of geological sensitive areas along the Budhi Khola Watershed, Sunsari/Morang districts, Eastern Nepal Himalaya. *Journal of Development Innovation* (Karma Quest International, Canada) **6**(1): 44-68. www.karmaquest.org/journal.
- Dahal, R. K., Hasegawa, S., Bhandary, N. P., Poudel, P. P., Nonomura, A. & Yatabe, R. (2012). A replication of landslide hazard mapping at catchment scale. *Geomatics, Natural Hazards, and Risk*, **3**(2): 161-192. <https://doi.org/10.1080/19475705.2011.629007>

- Dahal, R. K., Hasegawa, S., Nonomura, A., Yamanaka, M., Masuda, T. & Nishino, K. (2008). GIS-based weights-of-evidence modeling of rainfall-induced landslides in small catchments for landslide susceptibility mapping. *Environmental Geology* **54**(2): 311–324. <https://doi.org/10.1007/s00254-007-0818-3>
- Dai, F. C. & Lee, C. F. (2001). Terrain-based mapping of landslide susceptibility using a geographical information system: a case study. *Canadian Geotechnical Journal* **38**(9): 11-23. <https://doi.org/10.1139/t01-021>.
- Devkota, K. C., Regmi, A. D., Pourghasemi, H. R., Yoshida, K., Pradhan, B., Ryu, I. C. *et al.* (2012). Landslide susceptibility mapping using certainty factor, index of entropy, and logistic regression models in Geographical Information System (GIS) and their comparison at Mugling–Narayanghat Road section in Nepal Himalaya. *Natural Hazards* **65**(1): 135-165. <https://doi.org/10.1007/s11069-012-0347-6>.
- Dhital, M. R., 2000. An overview of landslide hazard mapping and rating systems in Nepal. *Jour of Nepal Geological Society* **22**: 533-538. <https://doi.org/10.3126/jngs.v22i0.32428>.
- Dhital, M. R. (2015). *Geology of the Nepal Himalaya:the regional perspective of the classic collided orogen*. Springer publication. <https://doi.org/10.1007/978-3-319-02496-7>.
- Hamza, T. & Raghuvanshi, T. K. (2017). GIS-based landslide hazard evaluation and zonation - A case from Jeldu district, central Ethiopia. *Journal of King Saud University* **29**(2): 151-65. <https://doi.org/10.1016/j.jksus.2016.05.002>.
- K.C., J., Gautam, D., Neupane, P. & Paudyal, K. R. (2018). Landslide inventory mapping and assessment along the Ramche-Jharlang area in Dhading, Rasuwa and Nuwakot districts, Lesser Himalaya Central Nepal. *Journal of Nepal Geological Society* **55**(1): 103–108. <https://doi.org/10.3126/jngs.v55i1.22798>
- Lee, S. & Talib, J. A. (2005). Probabilistic landslide susceptibility and factor effect analysis. *Environmental Geology* **47**: 982-990. <https://doi.org/10.1007/s00254-005-1228-z>
- Neupane. A. & Paudyal. K. R. (2021). Lithological control on landslide in the Siwalik section of the Lakhandehi Khola Watershed of Sarlahi district, south-eastern Nepal. *Journal of Development Innovations*, (Karma Quest International, Canada) **5**(2): 44-65.

- Pathak, D. (2016). Knowledge-based landslide susceptibility mapping in the Himalayas. *Geo-environmental Disasters* **3**(8): 1-11. <https://doi.org/10.1186/s40677-016-0042-0>
- Paudyal, K. R.; Devkota, K. C., Parajuli, B. P., Shakya, P. & Baskota, P. (2021). Landslide susceptibility assessment using open-source data in the far western Nepal Himalaya: Case studies from selected local level units. *Journal of Institute of Science and Technology* **26**(2): 31-42. <https://doi.org/10.3126/jist.v26i2.41327>
- Pradhan, U. M. S., Shrestha, R. B., KC, S. B. & Sharma, S. R. (2002). Geological map of petroleum exploration block 7, Malangwa, Central Nepal (Scale: 1:250,000/single page). Petroleum Exploration Promotion Project, Department of Mines and Geology, Lainchaur, Kathmandu, Nepal.
- Regmi, A. D., Devkota, K. C., Yoshida, K., Pradhan, B., Pourghasemi, H. R., Takashi, K. & Aykut, A. (2014). Application of frequency ratio, statistical index, and weights-of-evidence models and their comparison in landslide susceptibility mapping in Central Nepal Himalaya. *Arabian Journal of Geosciences* **7**: 725-742. <https://doi.org/10.1007/s12517-012-0807-z>.
- Sarkar, S., Roy, A. K. & Martha, T. R. (2013). Landslide susceptibility assessment using information value method in parts of Darjeeling Himalayas. *Journal Geol Soc India* **82**(4): 351-362. <https://doi.org/10.1007/s12594-013-0162-z>.
- Sah, R. B. (1999). Current understandings and existing problems on the stratigraphy of Nepal Himalaya. *Journal of SAN* **1**: 1-29, Central Department of Geology, Tribhuvan University, Kathmandu, Nepal.
- Shahi, Y. B., Kadel, S., Dangi, H., Adhikari, G., K. C. D., Paudyal, K. R. (2022). Geological exploration, landslide characterization, and susceptibility mapping at the boundary between two crystalline bodies in Jajarkot, Nepal. *Geotechnics* **2**: 1059-1083. <https://doi.org/10.3390/geotechnics2040050>
- Shano, L., Raghuvanshi, T. K & Meten, M. (2020). Landslide susceptibility evaluation and hazard zonation techniques-a review. *Geoenvirom Disasters* **7**: 18. <https://doi.org/10.1186/s40677-020-00152-0>.
- Thakur, V. C. (2001). *Regional geology and geological evolution of the Himalayas. Landslide problem mitigation to the Hindukush-Himalayas*, International Centre for Integrated Mountain Development publication. <https://doi.org/10.53055/ICIMOD.374>.
- Timalsina, K. & Paudyal, K. R. (2018). Fault-controlled geomorphic features in Ridi-Shantipur area of Gulmi District and their implications for active tectonics.

Journal of Nepal Geological Society **55**(1): 157–165. <https://doi.org/10.3126/jngs.v55i1.22807>

TU-CDES (2016). *Landslide Inventory Characterization and Engineering Design for Mitigation Works of Chure Area in Ten Districts*. Central Department of Environmental Science, Tribhuvan University and President Chure-Tarai Madhesh Conservation Development Board, Kathmandu. <https://doi.org/10.13140/RG.2.2.14028.31368>.

Upreti, B. N., & Dhital, M. R. (1996). *Landslide studies and management in Nepal*. International Centre for Integrated Mountain Development (ICIMOD), Kathmandu. <https://nppr.org.np/index.php/journal/article/view/43>.

Upreti, B. (2001). *The physiography and geology of Nepal and landslide hazards*. Landslide problem mitigation to the Hindukush-Himalayas, International Centre for Integrated Mountain Development publication. <https://doi.org/10.53055/ICIMOD.374>.